Hindawi Publishing Corporation
Mathematical Problems in Engineering
Volume 2013, Article ID 813904, 11 pages
http://dx.doi.org/10.1155/2013/813904

Research Article

A Systematic Approach for Calculating the Symbol Error Rate for the Entire Range of E_b/N_0 above and below the Threshold Point for the CE-OFDM System

Monika Pinchas and Yosef Pinhasi

Department of Electrical and Electronic Engineering, Ariel University Center of Samaria, 40700 Ariel, Israel

Correspondence should be addressed to Monika Pinchas; monika.pinchas@gmail.com

Received 4 October 2012; Accepted 2 December 2012

Academic Editor: Ming Li

Recently, the performance of the constant envelope OFDM (CE-OFDM) was analyzed in additive white Gaussian noise (AWGN) with the help of a closed-form approximated expression for the symbol error rate (SER). This expression was obtained with the assumption of having a high carrier-to-noise ratio (CNR) which, in effect, linearized the phase demodulator (the phase demodulator was implemented with an arctangent calculator) and simplified the analysis. Thus, this expression is not accurate for the lower range of CNR. As a matter of fact, it was already observed that there is a threshold point from which the simulated SER result vanishes from the theoretically obtained expression. In this paper, we present a systematic approach for calculating the SER without assuming having the high CNR case or using linearization techniques. In other words, we derive the SER for the nonlinear case. As a byproduct, we obtain a new closed-form approximated expression for the SER based on the Laplace integral method and the Edgeworth expansion. Simulation results indicate that the simulated results and those obtained from the new derived expression are very close for the entire range of bit energy-to-noise density ratio (E_b/N_0) above and below the threshold point.

1. Introduction

The orthogonal multicarrier modulation technique, also known as "orthogonal frequency division multiplexing" (OFDM) technique, is the standard modulation scheme used in Europe for Digital Audio Broadcasting (DAB) and Digital Video Broadcasting (DVB) [1–3]. In addition, local area networks (LANs) such as IEEE 802.11a are OFDM based [3]. OFDM is an excellent solution to the frequency selective fading problem in wireless applications [3]. However, spurious high amplitude peaks in the composite time signal occur when the signals from the different tones add constructively [4]. Compared to the average signal power, the instantaneous power of these peaks is high and, consequently, so is the peak-to-average power ratio (PAPR) [4]. The occurrence of these peaks seriously hampers practical implementations and is generally considered as one of the major drawbacks of OFDM [4]. Recently [5–8], the constant envelope OFDM (CE-OFDM) was proposed for solving the PAPR problem associated with OFDM. CE-OFDM transforms the OFDM signal, by way of phase modulation, to a signal designed for efficient power amplification [5]. At the receiver, the inverse transformation—phase demodulation—is applied prior to the conventional OFDM demodulator [5]. The performance of CE-OFDM was analyzed in [5] where a closed-form approximated expression was given for the SER for the AWGN channel case. However, this proposed expression for the SER [5] was obtained by assuming having high values for E_b/N_0 and by using linearization techniques to avoid the nonlinear problem caused by the phase demodulator (the phase demodulator was implemented with an arctangent calculator). Thus, it is accurate only for the higher range of E_b/N_0. It should be pointed out that it was already observed in [5] that the simulated SER results vanish from those obtained by the proposed expression for the SER for the lower range of E_b/N_0.

In the engineering field, it is very common to avoid the nonlinear problem caused by the phase demodulator

by assuming high E_b/N_0 and using linearization techniques [9, 10]. The main purpose of this paper is to show a systematic approach for calculating the SER without avoiding the nonlinear problem caused by the phase demodulator. As a byproduct, we obtain a new closed-form approximated expression for the SER that is valid for the entire range of E_b/N_0 and AWGN case. Namely, the new expression is valid also for the lower range of E_b/N_0. It is based on the Edgeworth expansion up to order four [11, 12], Laplace integral method (see [13, page. 261–274], [3, 12, 14]), and is obtained without using linearization techniques.

The paper is organized as follows: after having described the system under consideration in Section 2, we introduce in Section 3 our systematic approach for calculating the SER. In Section 4 we present simulation results, and Section 5 is our conclusion.

2. System Description

The system under consideration is described in Figure 1 which is similar to that described in [5] for the AWGN case.

During each T-second block interval, an N_{DFT}-point inverse discrete Fourier transform (IDFT) calculates a block of time samples $x[n]$ where the input to the IDFT is a conjugate symmetric data vector $[0, X[1], X[2], \ldots, X[N_{\mathrm{QAM}}], \quad 0, X^*[N_{\mathrm{QAM}}], \ldots, X^*[2], X^*[1]]$ where $\{X[k]\}_{k=1}^{N_{\mathrm{QAM}}}$ are M_{QAM}-QAM data symbols and $(\cdot)^*$ is the conjugate operator on $(\cdot)$. The total length of the IDFT is equal to $2N_{\mathrm{QAM}} + 2$ and is defined in the following as N_{DFT}. In addition, we denote $N = 2N_{\mathrm{QAM}}$. The samples $x[n]$

$$\begin{aligned} x[n] &= \sum_{k=0}^{N_{\mathrm{DFT}}-1} X[k] \exp\left(j\frac{2\pi kn}{N_{\mathrm{DFT}}}\right) \\ &= 2\sum_{k=1}^{N_{\mathrm{QAM}}} \mathrm{Re}(X[k]) \cos\left(\frac{2\pi kn}{N_{\mathrm{DFT}}}\right) \\ &\quad - \mathrm{Im}(X[k]) \sin\left(\frac{2\pi kn}{N_{\mathrm{DFT}}}\right) \\ &\quad \text{for } n = 0, 1, 2, \ldots, N_{\mathrm{DFT}} - 1 \end{aligned} \tag{1}$$

are sent to the phase modulator to obtain the output signal $s[n]$ defined by

$$s[n] = \exp\left(j2\pi hCx[n]\right), \tag{2}$$

where h is the modulation index, $j = \sqrt{-1}$, $\mathrm{Re}(\cdot)$ and $\mathrm{Im}(\cdot)$ are the real and imaginary parts of $(\cdot)$, respectively, and C is defined by

$$C = \sqrt{\frac{1}{2N\sigma_I^2}}, \tag{3}$$

where $\sigma_I^2 = (M^2 - 1)/3$ and $M = \sqrt{M_{\mathrm{QAM}}}$. According to [5], the phase modulating OFDM signal is comprised of $N = 2N_{\mathrm{QAM}}$ subcarriers, each modulated by $M = \sqrt{M_{\mathrm{QAM}}}$-ary pulse amplitude modulation (PAM) data symbols $(\pm 1, \pm 3, \ldots, \pm(M-1))$.

Next, a cyclic prefix (CP) is appended to the sequence $s[n]$. The discrete-time samples are then passed through a digital-to-analog (D/A) converter, and the result is amplified and transmitted into the channel where it is corrupted by an additive white Gaussian noise $n(t)$. The received signal is $r(t) = s(t) + n(t)$ where $s(t) = A_s \exp(j2\pi hCx(t))$, $-T_{\mathrm{CP}} \le t < T$, T_{CP} is the cyclic prefix duration and A_s is the signal amplitude. This signal $(r(t))$ is then passed through an analog-to-digital (A/D) converter and after that sent to the block that discards the cyclic prefix samples. The samples that remain, $\hat{s}[n]$, are sent to the phase demodulator. The phase demodulator is implemented with an arctangent calculator followed by a phase unwrapper. The output of the phase demodulator is given by $\hat{\phi}[n] = \phi[n] + \xi[n]$ where $\xi[n]$ is a nonlinear noise component and $\phi[n] = 2\pi hCx[n]$. Next, the sequence $\hat{\phi}[n]$ is sent to the N_{DFT}-point DFT block to obtain

$$\begin{aligned} \widetilde{Q}[k] &= \frac{1}{N_{\mathrm{DFT}}} \sum_{n=0}^{N_{\mathrm{DFT}}-1} \hat{\phi}[n] \exp\left(-j\frac{2\pi kn}{N_{\mathrm{DFT}}}\right) \\ &= \frac{1}{N_{\mathrm{DFT}}} \sum_{n=0}^{N_{\mathrm{DFT}}-1} \phi[n] \exp\left(-j\frac{2\pi kn}{N_{\mathrm{DFT}}}\right) + \widetilde{N}[k] \\ &= 2\pi hCX[k] + \widetilde{N}[k], \end{aligned} \tag{4}$$

where $\widetilde{N}[k]$ is defined by

$$\widetilde{N}[k] = \frac{1}{N_{\mathrm{DFT}}} \sum_{n=0}^{N_{\mathrm{DFT}}-1} \xi[n] \exp\left(-j\frac{2\pi kn}{N_{\mathrm{DFT}}}\right). \tag{5}$$

Next, the vector $[\mathrm{Re}(\widetilde{Q}[k])\ \mathrm{Im}(\widetilde{Q}[k])]$ is sent to the symbol demapper that yields the received bits. Since the vector $[\mathrm{Re}(\widetilde{Q}[k])\ \mathrm{Im}(\widetilde{Q}[k])]$ is sent to the symbol demapper, the noise component we are interested in is defined by

$$N[k] = \frac{1}{N_{\mathrm{DFT}}} \sum_{n=0}^{N_{\mathrm{DFT}}-1} \frac{\xi[n]}{\sqrt{2}} \exp\left(-j\frac{2\pi kn}{N_{\mathrm{DFT}}}\right). \tag{6}$$

3. The Systematic Approach for Calculating the SER

Recently [5], the performance of CE-OFDM was analyzed in an AWGN channel where a closed-form approximated expression was given for the SER given by

$$\begin{aligned} \mathrm{SER} &\simeq 2\frac{M-1}{M} Q\left(2\pi h\sqrt{\frac{6(\log_2 M)}{(M^2-1)}\frac{E_b}{N_0}}\right), \\ \text{where} \quad Q(x) &= \frac{1}{\sqrt{2\pi}} \int_x^{\infty} e^{-u^2/2} du. \end{aligned} \tag{7}$$

As already mentioned earlier, this expression (7) was obtained by assuming the high E_b/N_0 case and using linearization

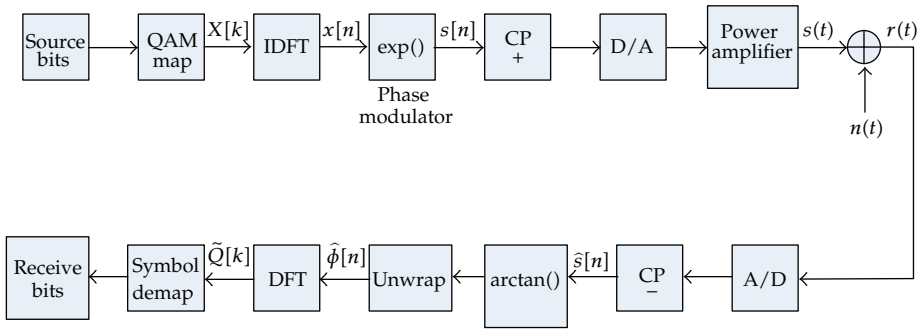

Figure 1: System description.

techniques. Thus, avoiding the nonlinear problem caused by the phase demodulator. In this section, we show a systematic approach for calculating the SER applicable for CE-OFDM system valid for the entire range of E_b/N_0 without using linearization techniques or avoiding the nonlinear problem caused by the phase demodulator. According to Figure 1, the CE-OFDM demodulator operates in the discrete-time domain. It is convenient, however, to consider the continuous-time model for analysis [5]. When no phase offset is caused by the channel, the output of the phase demodulator for the simple AWGN case is according to [5]

$$\widehat{\phi}(t) = \phi(t) + \xi(t), \tag{8}$$

where

$$\xi(t) = \arctan\left(\frac{A_n(t)\sin(\psi(t) - \phi(t))}{A_s + A_n(t)(\cos(\psi(t) - \phi(t)))}\right) \tag{9}$$

is a nonlinear noise component, $A_n(t) = |n(t)|$ (where $|\cdot|$ is the absolute function of $(\cdot)$), and $\psi(t)$ is the phase of $n(t)$.

Theorem 1. *For the following assumptions,*

(1) $E[n(t)] = 0$, $E[n(t)(n^*(t))] = \sigma_n^2$,

where $(\cdot)^*$ is the conjugate operation on $(\cdot)$ and $E[\cdot]$ is the expectation operator,

(2) $E[A_n(t)\sin(\psi(t)-\phi(t))] = E[A_n(t)\cos(\psi(t)-\phi(t))] = 0$,

(3) $E[(A_n(t)\sin(\psi(t) - \phi(t)))^2] = E[(A_n(t)\cos(\psi(t) - \phi(t)))^2] = \sigma_n^2/2$,

(4) $A_n(t)\sin(\psi(t) - \phi(t))$ *and* $A_n(t)\cos(\psi(t) - \phi(t))$ *are Gaussian processes,*

the SER is approximately given by

$$\begin{aligned} SER \simeq{}& 2\left(\frac{M-1}{M}\right)Q\left(\frac{d}{\sigma_N}\right) + 2\left(\frac{M-1}{M}\right) \\ &\times 3\frac{E\left[N^4[k]\right] - 3\left(\sigma_N^2\right)^2}{4!\left(\sigma_N^2\right)^2}Q\left(\frac{d}{\sigma_N}\right) \\ &+ 2\left(\frac{M-1}{M}\right)\frac{E\left[N^4[k]\right] - 3\left(\sigma_N^2\right)^2}{4!\left(\sigma_N^2\right)^4} \\ &\times\left[\frac{1}{4}\frac{\sqrt{2}}{\sqrt{\pi}}\sigma_N\left(2d^3e^{-(1/2)(d^2/\sigma_N^2)}\right.\right. \\ &\left.\left.+6d\sigma_N^2e^{-(1/2)(d^2/\sigma_N^2)}\right) + 3\sigma_N^4Q\left(\frac{d}{\sigma_N}\right)\right] \\ &- 2\left(\frac{M-1}{M}\right)6\frac{E\left[N^4[k]\right] - 3\left(\sigma_N^2\right)^2}{4!\left(\sigma_N^2\right)^2} \\ &\times\frac{1}{\sqrt{2\pi}}\left[\frac{d}{\sigma_N}e^{-(d/\sigma_N)^2/2} + \sqrt{2\pi}Q\left(\frac{d}{\sigma_N}\right)\right], \end{aligned} \tag{10}$$

where

$$\begin{aligned} \sigma_N^2 \simeq{}& \frac{1}{4N(\log_2 M)(E_b/N_0)}\left(1 + \frac{N_{DFT}}{2N(\log_2 M)(E_b/N_0)}\right) \\ &+ \frac{1}{24N_{DFT}}\pi^2e^{-(N/N_{DFT})(\log_2 M)(E_b/N_0)}, \end{aligned} \tag{11}$$

$$\begin{aligned} E\left[N^4[k]\right] \simeq{}& \frac{3}{16}\left(\frac{1}{N(\log_2 M)(E_b/N_0)}\right)^2 \\ &\times\left(1 + \frac{5}{3}\left(\frac{N_{DFT}}{N(\log_2 M)(E_b/N_0)}\right)\right) \\ &+ \frac{1}{320N_{DFT}^2}\pi^4e^{-(N/N_{DFT})(\log_2 M)(E_b/N_0)}, \end{aligned} \tag{12}$$

$$Q\left(\frac{d}{\sigma_N}\right) = \frac{1}{\sqrt{2\pi}}\int_{d/\sigma_N}^{\infty} e^{-u^2/2}du, \tag{13}$$

$$d = 2\pi h\sqrt{\frac{1}{2N\sigma_I^2}} \tag{14}$$

and $! = 1\cdot 2\cdot 3\cdot\cdots\cdot(n-1)$, $0! = 1$.

Proof. According to [15], the symbol error rate is computed by determining the probability of error for each signal point in the M-PAM constellation. For the M-2 inner points, the probability of error is

$$P_{\text{inner}} = P\left(|N[k]| > d\right) = 2P\left(N[k] > d\right), \tag{15}$$

where $d = 2\pi h\sqrt{1/2N\sigma_I^2}$ as given in (14). For the two outer points, the probability of error is [15]

$$P_{\text{outer}} = P\left(N[k] > d\right) = \frac{P_{\text{inner}}}{2}. \tag{16}$$

Therefore, the overall symbol error rate is [15]

$$\begin{aligned}\text{SER} &= \frac{M-2}{M}P_{\text{inner}} + \frac{2}{M}P_{\text{outer}}\\ &= \frac{M-2}{M}P_{\text{inner}} + \frac{1}{M}P_{\text{inner}} = \frac{M-1}{M}P_{\text{inner}}.\end{aligned} \tag{17}$$

Now, in order to calculate the probability that $N[k] > d$ (15), the probability density function (pdf) of $N[k]$ is needed. Since we do not know the pdf of $N[k]$, we use the Edgeworth expansion up to order four [11, 12] for approximating it:

$$\begin{aligned}\widehat{f}\left(N[k]\right) \simeq{}& \frac{1}{\sqrt{2\pi}\sigma_N}e^{-N^2[k]/2\sigma_N^2}\\ &\times\left[1 + \left(\frac{E\left[N^4[k]\right] - 3\left(\sigma_N^2\right)^2}{4!\left(\sigma_N^2\right)^2}\right)\right.\\ &\left.\times\left(\frac{N^4[k]}{\left(\sigma_N^2\right)^2} - \frac{6N^2[k]}{\sigma_N^2} + 3\right)\right],\end{aligned} \tag{18}$$

where $E[N^2[k]] = \sigma_N^2$. According to (6), $N[k]$ is a function of the random variable $\xi[n]$. Thus, having the statistics of $\xi(t)$, namely, by knowing the following expressions $E[(\xi(t))^2]$ and $E[(\xi(t))^4]$, the approximated pdf for $N[k]$ (18) is well defined.

Theorem 2. $E[(\xi(t))^2]$ *and* $E[(\xi(t))^4]$ *may be given by*

$$\begin{aligned}E\left[(\xi(t))^2\right] &\simeq \frac{\sigma_n^2}{2a^2}\left(1 + \frac{\sigma_n^2}{2a^2}\right) + \frac{1}{12}\pi^2 e^{-(a^2/\sigma_n^2)},\\ E\left[(\xi(t))^4\right] &\simeq \frac{5}{4}\left(\frac{\sigma_n^2}{a^2}\right)^3 + \frac{3}{4}\left(\frac{\sigma_n^2}{a^2}\right)^2 + \frac{1}{80}\pi^4 e^{-(a^2/\sigma_n^2)},\end{aligned} \tag{19}$$

where

$$\frac{\sigma_n^2}{a^2} = \frac{N_{DFT}}{N\log_2(M)\left(E_b/N_0\right)}. \tag{20}$$

Proof. Let us rewrite (9) as

$$\xi(t) = \arctan\left(\frac{x}{a+y}\right), \tag{21}$$

where $a = A_s$, $x = A_w(t)\sin(\psi(t) - \phi(t))$ and $y = A_w(t)(\cos(\psi(t) - \phi(t)))$. According to [3, 16], the pdf of the random variable $\xi(t)$ is given for $|\xi(t)| < \pi/2$ by

$$\begin{aligned}f\left(\xi(t)\right) ={}& \frac{\exp\left(-1/\rho\right)}{\pi}\\ &+ \frac{\sqrt{2/\rho}\cos\left(\xi(t)\right)\exp\left(-\sin^2\left(\xi(t)\right)/\rho\right)}{\sqrt{\pi/2}}\\ &\times \operatorname{erf}\left(\sqrt{\frac{2}{\rho}}\cos\left(\xi(t)\right)\right),\end{aligned} \tag{22}$$

where $\rho = 2(\sigma_n^2/2)/a^2 = \sigma_n^2/a^2$ and $\operatorname{erf}(x) = (1/\sqrt{2\pi})\int_0^x \exp(-y^2/2)dy$. Next, we recall from [3] the derived expression for $E[(\xi(t))^2]$ based on (22):

$$E\left[(\xi(t))^2\right] \simeq \frac{\sigma_n^2}{2a^2}\left(1 + \frac{\sigma_n^2}{2a^2}\right) + \frac{1}{12}\pi^2 e^{-(a^2/\sigma_n^2)}, \tag{23}$$

thus leaving us now only with the derivation of $E[(\xi(t))^4]$ defined by

$$\begin{aligned}&E\left[(\xi(t))^4\right]\\ &= \int_{-\pi/2+\varepsilon}^{\pi/2-\varepsilon}\xi^4(t)\,f\left(\xi(t)\right)d\xi(t)\\ &= \int_{-\pi/2+\varepsilon}^{\pi/2-\varepsilon}\xi^4(t)\left[\frac{\exp\left(-1/\rho\right)}{\pi}\right.\\ &\qquad + \frac{\sqrt{2/\rho}\cos\left(\xi(t)\right)\exp\left(-\sin^2\left(\xi(t)\right)/\rho\right)}{\sqrt{\pi/2}}\\ &\qquad \left.\times\operatorname{erf}\left(\sqrt{2/\rho}\cos\left(\xi(t)\right)\right)\right]d\xi(t),\end{aligned} \tag{24}$$

which we split into two integrals:

$$E\left[(\xi(t))^4\right] = I_1 + I_2, \tag{25}$$

where

$$I_1 = \int_{-\pi/2+\varepsilon}^{\pi/2-\varepsilon}\xi^4(t)\frac{\exp\left(-1/\rho\right)}{\pi}d\xi(t), \tag{26}$$

$$\begin{aligned}I_2 ={}& \int_{-(\pi/2)+\varepsilon}^{(\pi/2)-\varepsilon}\xi^4(t)\frac{\sqrt{2/\rho}\cos\left(\xi(t)\right)\exp\left(-\sin^2\left(\xi(t)\right)/\rho\right)}{\sqrt{\pi/2}}\\ &\times\operatorname{erf}\left(\sqrt{\frac{2}{\rho}}\cos\left(\xi(t)\right)\right)d\xi(t),\end{aligned} \tag{27}$$

and ε is a small fixed positive value. Now, if we define

$$\Psi(\xi(t)) = \sin^2(\xi(t)),$$
$$f(\xi(t)) = \frac{\sqrt{2/\rho}\cos(\xi(t))\,\xi^4(t)}{\sqrt{\pi/2}}\operatorname{erf}\left(\sqrt{\frac{2}{\rho}}\cos(\xi(t))\right), \tag{28}$$

we obtain, by using (28) and (27):

$$I_2 = \int_{-\pi/2+\varepsilon}^{\pi/2-\varepsilon} f(\xi(t))\exp\left(-\frac{\Psi(\xi(t))}{\rho}\right)d\xi(t). \tag{29}$$

In order to solve (29), we use the Laplace integral method following [3]. According to [3], the Laplace method [13, page. 261–274] is a very general technique for obtaining the asymptotic behavior as $\rho \to 0$ of integrals in which the large parameter $1/\rho$ appears in the exponent. The main idea of Laplace's method [13, page. 261–274] is to use the fact that if the real continuous function $\Psi(\xi(t))$ has its minimum at $\xi_0(t)$, which is between infinity and minus infinity, then it is only the immediate neighborhood of $\xi(t) = \xi_0(t)$ that contributes to the full asymptotic expansion of the integral (29) for large $1/\rho$. The function $\Psi(\xi(t))$ has its minimum at $\xi(t) = 0$. Therefore, for $\rho \to 0$ and for the immediate neighborhood of $\xi(t) = 0$, we may write, as was done in [3],

$$\operatorname{erf}\left(\sqrt{\frac{2}{\rho}}\cos(\xi(t))\right) \cong \operatorname{erf}\left(\sqrt{\frac{2}{\rho}}\right) \cong 0.5. \tag{30}$$

Using the Laplace Integral method [13, page. 261–274] and (30) we may approximate (29) in the following way

$$I_2 \simeq \sqrt{\frac{2}{\rho}}\int_{\xi_0(t)-\varepsilon_1}^{\xi_0(t)+\varepsilon_1} f_1(\xi(t))\exp\left(-\frac{\Psi(\xi(t))}{\rho}\right)d\xi(t), \tag{31}$$

where

$$f_1(\xi(t)) = \frac{\cos(\xi(t))\,\xi^4(t)}{2\sqrt{\pi/2}}, \tag{32}$$

$\xi_0(t)$ is the point where the function $\Psi(\xi(t))$ has its minimum and ε_1 is a small fixed positive value. According to the Laplace Integral method [13, page. 261–274] and [3], we may write (31) in the following way

$$\begin{aligned} I_2 \simeq{}& \sqrt{\frac{2}{\rho}}\exp\left(-\frac{\Psi(\xi_0(t))}{\rho}\right)\sqrt{\frac{2\pi\rho}{\Psi''(\xi_0(t))}} \\ &\cdot\left[f_1(\xi_0(t)) + \frac{f_1''(\xi_0(t))}{2}\frac{\rho}{\Psi''(\xi_0(t))}\right. \\ &+ \frac{f_1^{IV}(\xi_0(t))}{8}\left(\frac{\rho}{\Psi''(\xi_0(t))}\right)^2 \\ &+ \frac{-\Psi^{IV}(\xi_0(t))}{48\rho}f_1''(\xi_0(t))\,15\left(\frac{\rho}{\Psi''(\xi_0(t))}\right)^3 \\ &+ \frac{-\Psi^{IV}(\xi_0(t))}{(24)^2\rho}f_1^{IV}(\xi_0(t))\,105\left(\frac{\rho}{\Psi''(\xi_0(t))}\right)^4 \\ &\left.+ \frac{f_1^{VI}(\xi_0(t))}{720}15\left(\frac{\rho}{\Psi''(\xi_0(t))}\right)^3\right], \end{aligned} \tag{33}$$

where $f_1^{(n)}(\xi_0(t))$ and $\Psi^{(n)}(\xi_0(t))$ are the nth derivation of f_1 and Ψ, respectively, at the minimum point $\xi_0(t) = 0$ and $O(x)$ is defined as $\lim_{x\to 0}(O(x)/x) = r$, where "$r$" is a constant value. Next, we derive the second, fourth, and sixth derivative of $f_1(\xi(t))$ at the minimum point $\xi_0(t) = 0$:

$$\begin{aligned} f_1''(\xi(t)) = {}& -\frac{1}{2\sqrt{\pi}}\left(\sqrt{2}(\xi(t))^4\cos\xi(t)\right. \\ &- 12\sqrt{2}(\xi(t))^2\cos\xi(t) \\ &\left.+8\sqrt{2}(\xi(t))^3\sin\xi(t)\right) \\ &\Downarrow \\ & f_1''(\xi_0(t)) = 0, \end{aligned}$$

$$\begin{aligned} & f_1^{IV}(\xi(t)) \\ &= \frac{1}{2\sqrt{\pi}}\left(24\sqrt{2}\cos\xi(t) - 72\sqrt{2}(\xi(t))^2\cos\xi(t)\right. \\ &\quad + \sqrt{2}(\xi(t))^4\cos\xi(t) + 16\sqrt{2}(\xi(t))^3\sin\xi(t) \\ &\quad \left.-96\sqrt{2}\xi(t)\sin\xi(t)\right) \\ &\qquad \Downarrow \\ &\qquad f_1^{IV}(\xi_0(t)) = \frac{1}{2\sqrt{\pi}}24\sqrt{2}, \end{aligned}$$

$$\begin{aligned} & f_1^{VI}(\xi(t)) \\ & = -\frac{1}{2\sqrt{\pi}}\Big(360\sqrt{2}\cos\xi(t) - 180\sqrt{2}(\xi(t))^2\cos\xi(t) \\ & \quad + \sqrt{2}(\xi(t))^4\cos\xi(t) + 24\sqrt{2}(\xi(t))^3\sin\xi(t) \\ & \quad -480\sqrt{2}\xi(t)\sin\xi(t)\Big) \\ & \quad \Downarrow \\ & \quad f_1^{VI}(\xi_0(t)) = -\frac{1}{2\sqrt{\pi}}360\sqrt{2}. \end{aligned} \tag{34}$$

By substituting (34), $\Psi''(\xi_0(t)) = 2$, $\Psi^{IV}(\xi_0(t)) = -8$, and $f_1(\xi_0(t)) = 0$ into (33), we obtain

$$\begin{aligned} I_2 \simeq \ & \sqrt{2\pi}\Bigg(\frac{(1/2\sqrt{\pi})(24\sqrt{2})}{8}\left(\frac{\rho}{2}\right)^2 \\ & + \frac{8}{(24)^2\rho}\frac{1}{2\sqrt{\pi}}(24\sqrt{2})105\left(\frac{\rho}{2}\right)^4 \\ & - \frac{1}{2\sqrt{\pi}}360\sqrt{2}\frac{1}{720}15\left(\frac{\rho}{2}\right)^3\Bigg) \\ & \Downarrow \\ & I_2 \simeq \frac{5}{4}\rho^3 + \frac{3}{4}\rho^2. \end{aligned} \tag{35}$$

Next, we calculate I_1:

$$I_1 = \int_{-\pi/2+\varepsilon}^{\pi/2-\varepsilon} \xi^4(t)\frac{\exp(-1/\rho)}{\pi}d\xi(t) = \frac{1}{80}\pi^4 e^{-1/\rho}. \tag{36}$$

We have already mentioned earlier that $\rho = \sigma_n^2/a^2$. Thus, our next task is to find a closed expression for σ_n^2/a^2 as a function of E_b/N_0 and the various system parameters used such as the number of useful carriers (N), number of total carriers (N_{DFT}), and the order of the PAM modulation used (M). For our case, the expression for E_b/N_0 can be written by

$$\begin{aligned} & \frac{E_b}{N_0} = \frac{E_s/N_0}{N\log_2(M)} = \frac{a^2 N_{\mathrm{DFT}} T_s}{N_0 N\log_2(M)} \\ & \Downarrow \\ & N_0 = \frac{a^2 N_{\mathrm{DFT}} T_s}{N\log_2(M)(E_b/N_0)}, \end{aligned} \tag{37}$$

where $1/T_s$ is the frequency sampling rate and $T = N_{\mathrm{DFT}}T_s$. Now, by using (37), we may define σ_n^2 as

$$\sigma_n^2 = \frac{N_0}{T_s} = \frac{a^2 N_{\mathrm{DFT}}}{N\log_2(M)(E_b/N_0)}. \tag{38}$$

Next, by dividing both sides of (38) by a^2, the expression of (20) is obtained. By using now $\rho = \sigma_n^2/a^2$, (38), (36), (35), and (23), we obtain (19). This completes the proof of Theorem 2.

Now, we turn to calculate $E[N^2[k]]$ and $E[N^4[k]]$. By using (6) and the property of $E[\xi[n]\xi[m]] = E[\xi^2[n]]\delta[n-m]$, we obtain

$$\begin{aligned} E\left[N^2[k]\right] &= \frac{1}{2N_{\mathrm{DFT}}^2}\sum_{n=0}^{N_{\mathrm{DFT}}-1}\sum_{m=0}^{N_{\mathrm{DFT}}-1} E\left[\xi[n]\xi[m]\right] \\ &\quad \times \exp\left(\frac{-j2\pi kn}{N_{\mathrm{DFT}}}\right)\exp\left(\frac{-j2\pi km}{N_{\mathrm{DFT}}}\right) \\ &= \frac{1}{2N_{\mathrm{DFT}}}E\left[\xi^2[n]\right], \\ E\left[N^4[k]\right] &= \frac{1}{4N_{\mathrm{DFT}}^4}\sum_{n=0}^{N_{\mathrm{DFT}}-1}\sum_{m=0}^{N_{\mathrm{DFT}}-1}\sum_{\check{n}=0}^{N_{\mathrm{DFT}}-1}\sum_{\check{m}=0}^{N_{\mathrm{DFT}}-1} \\ &\quad \cdot E\left[\xi[n]\xi[m]\xi[\check{n}]\xi[\check{m}]\right]\exp\left(\frac{-j2\pi kn}{N_{\mathrm{DFT}}}\right) \\ &\quad \times \exp\left(\frac{-j2\pi km}{N_{\mathrm{DFT}}}\right)\exp\left(\frac{-j2\pi k\check{n}}{N_{\mathrm{DFT}}}\right) \\ &\quad \times \exp\left(\frac{-j2\pi k\check{m}}{N_{\mathrm{DFT}}}\right) \\ &\cong \frac{1}{4N_{\mathrm{DFT}}^2}E\left[\xi^4[n]\right]. \end{aligned} \tag{39}$$

By substituting (20) and (19) into (39), the expressions for $E[N^2[k]]$ and $E[N^4[k]]$ given in (11) and (12), respectively, are obtained. Now, we are ready to carry out the calculation of the probability that $N[k] > d$ which is needed in (15). By using the estimated pdf of $N[k]$ (18), the probability that $N[k] > d$ is defined by

$$\begin{aligned} & P(N[k] > d) \\ & \simeq \int_d^{\infty}\frac{1}{\sqrt{2\pi}\sigma_N}e^{-(N^2[k]/2\sigma_N^2)} \\ & \quad \times\left[1 + H\left(\frac{N^4[k]}{(\sigma_N^2)^2} - \frac{6N^2[k]}{\sigma_N^2} + 3\right)\right]dN, \text{where,} \\ & \quad H = \frac{E\left[N^4[k]\right] - 3\left(\sigma_N^2\right)^2}{4!(\sigma_N^2)^2}. \end{aligned} \tag{40}$$

In order to find a solution for (40), the following integrals are first carried out: $\int_d^{\infty}(1/\sqrt{2\pi}\sigma_N)e^{-(N^2[k]/2\sigma_N^2)}dN[k]$, $\int_d^{\infty}N^2[k](1/\sqrt{2\pi}\sigma_N)e^{-(N^2[k]/2\sigma_N^2)}dN[k]$, and $\int_d^{\infty}N^4[k](1/\sqrt{2\pi}\sigma_N)e^{-(N^2[k]/2\sigma_N^2)}dN[k]$.

By using $N[k]/\sigma_N = u$ and $dN[k]/\sigma_N = du$, we may write

$$\begin{aligned}
&\int_d^\infty \frac{1}{\sqrt{2\pi}\sigma_N} e^{-N^2[k]/2\sigma_N^2} dN[k] \\
&\quad = \frac{1}{\sqrt{2\pi}} \int_{d/\sigma_N}^\infty e^{-u^2/2} du = Q\left(\frac{d}{\sigma_N}\right), \\
&\int_d^\infty N^2[k] \frac{1}{\sqrt{2\pi}\sigma_N} e^{-N^2[k]/2\sigma_N^2} dN[k] \\
&\quad = \frac{\sigma_N^2}{\sqrt{2\pi}} \int_{d/\sigma_N}^\infty u^2 e^{-u^2/2} du \\
&\quad = \frac{\sigma_N^2}{\sqrt{2\pi}} \left[\int_0^\infty u^2 e^{-u^2/2} du - \int_0^{d/\sigma_N} u^2 e^{-u^2/2} du\right] \\
&\quad = \frac{\sigma_N^2}{\sqrt{2\pi}} \left[\frac{d}{\sigma_N} e^{-(d/\sigma_N)^2/2} + \sqrt{2\pi} Q\left(\frac{d}{\sigma_N}\right)\right], \\
&\int_d^\infty N^4[k] \frac{1}{\sqrt{2\pi}\sigma_N} e^{-N^2[k]/2\sigma_N^2} dN[k] \\
&\quad = \frac{\sigma_N^4}{\sqrt{2\pi}} \int_{d/\sigma_N}^\infty u^4 e^{-u^2/2} du \\
&\quad = \frac{1}{4}\frac{\sqrt{2}}{\sqrt{\pi}} \sigma_N \left(2d^3 e^{-(1/2)(d^2/\sigma_N^2)} + 6d\sigma_N^2 e^{-(1/2)(d^2/\sigma_N^2)}\right) \\
&\qquad + 3\sigma_N^4 Q\left(\frac{d}{\sigma_N}\right).
\end{aligned} \tag{41}$$

Now, by substituting (41) into (40), we obtain

$$\begin{aligned}
P(N[k] > d) \simeq{}& \left[1 + 3\frac{E\left[N^4[k]\right] - 3\left(\sigma_N^2\right)^2}{4!\left(\sigma_N^2\right)^2}\right] Q\left(\frac{d}{\sigma_N}\right) \\
&+ \frac{E\left[N^4[k]\right] - 3\left(\sigma_N^2\right)^2}{4!\left(\sigma_N^2\right)^4} \\
&\times \left[\frac{1}{4}\frac{\sqrt{2}}{\sqrt{\pi}}\sigma_N \left(2d^3 e^{-(1/2)(d^2/\sigma_N^2)}\right.\right. \\
&\qquad \left.\left. + 6d\sigma_N^2 e^{-(1/2)(d^2/\sigma_N^2)}\right) \right. \\
&\qquad \left. + 3\sigma_N^4 Q\left(\frac{d}{\sigma_N}\right)\right] \\
&- 6\frac{E\left[N^4[k]\right] - 3\left(\sigma_N^2\right)^2}{4!\left(\sigma_N^2\right)^2} \frac{1}{\sqrt{2\pi}} \\
&\times \left[\frac{d}{\sigma_N} e^{-(d/\sigma_N)^2/2} + \sqrt{2\pi} Q\left(\frac{d}{\sigma_N}\right)\right].
\end{aligned} \tag{42}$$

Next, by using (42), (17), and (15), the expression of (10) is obtained. This completes the proof of Theorem 1. □

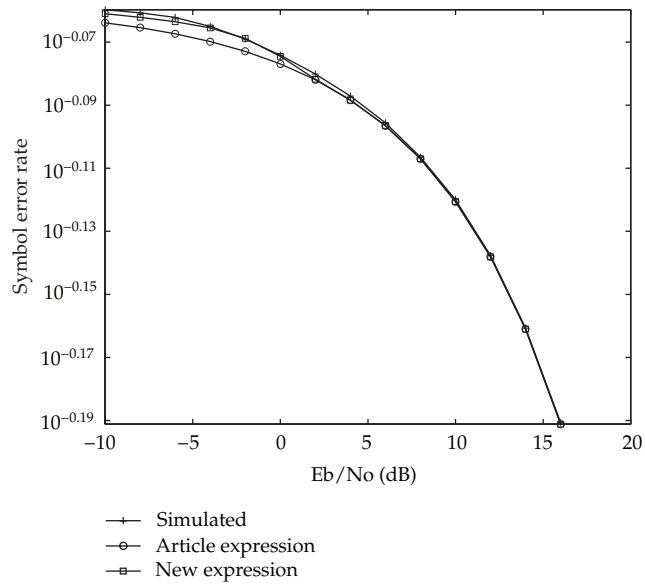

Figure 2: SER comparison as a function of E_b/N_0 between the simulated, new proposed expression (10) and the expression proposed by [5] given in (7). $N_{\mathrm{DFT}} = 64$, $h = 0.1/2\pi$, $A_s = 2$, modulation type: $M = 8$. The averaged results were obtained in 100 Monte Carlo trials where 500 CE-OFDM signals were produced for each trial.

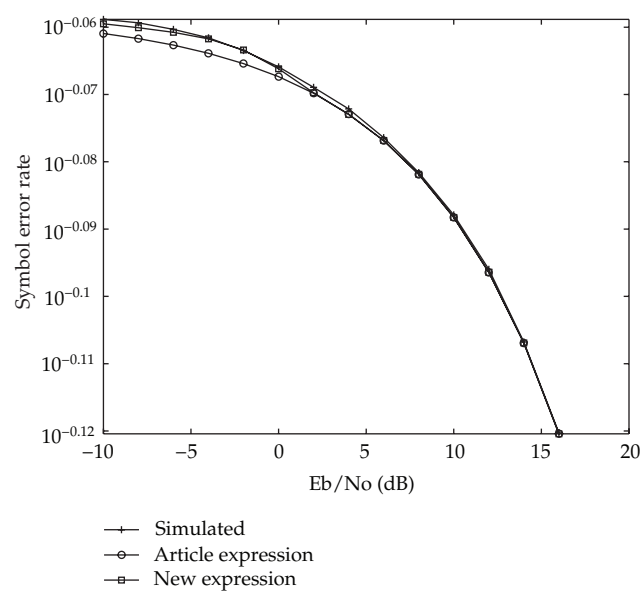

Figure 3: SER comparison as a function of E_b/N_0 between the simulated, new proposed expression (10) and the expression proposed by [5] given in (7). $N_{\mathrm{DFT}} = 64$, $h = 0.05/2\pi$, $A_s = 2$, modulation type: $M = 8$. The averaged results were obtained in 100 Monte Carlo trials where 500 CE-OFDM signals were produced for each trial.

4. Simulation

In this section, we test the new obtained expression for the SER (10) for the $M = 2$ and $M = 8$ case with DFT length of $N_{\mathrm{DFT}} = 8, 32, 64$ for a wide range of E_b/N_0 values. The results are compared with those obtained from (7) and with

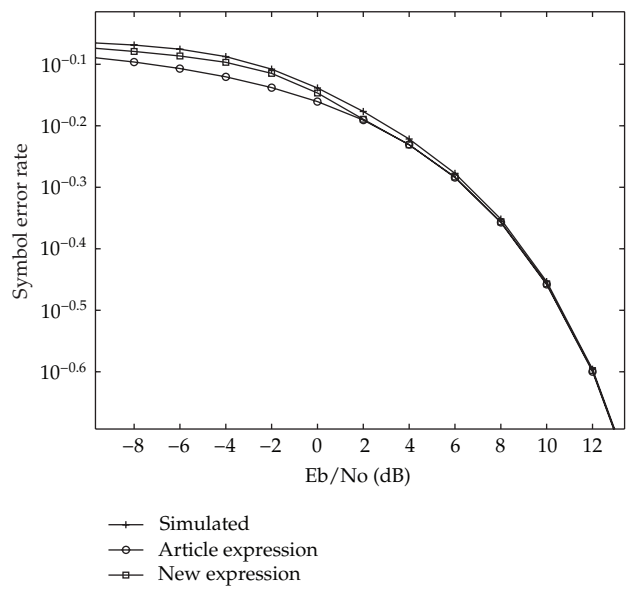

Figure 4: SER comparison as a function of E_b/N_0 between the simulated, new proposed expression (10) and the expression proposed by [5] given in (7). $N_{\mathrm{DFT}} = 64$, $h = 0.5/2\pi$, $A_s = 2$, modulation type: $M = 8$. The averaged results were obtained in 100 Monte Carlo trials where 500 CE-OFDM signals were produced for each trial.

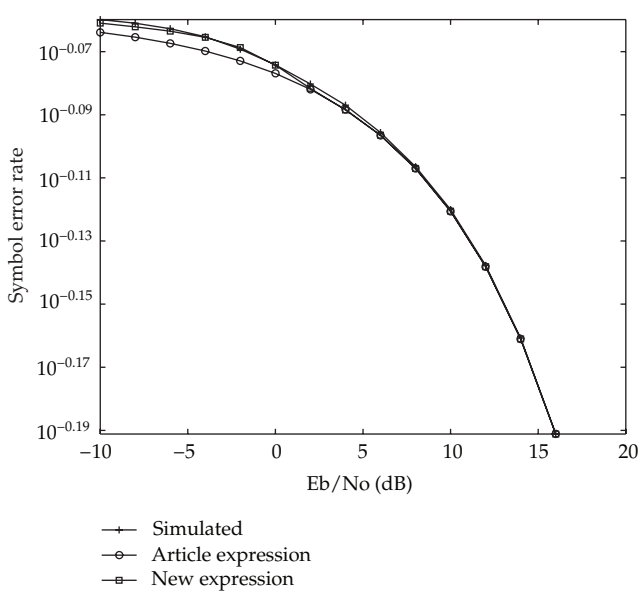

Figure 5: SER comparison as a function of E_b/N_0 between the simulated, new proposed expression (10) and the expression proposed by [5] given in (7). $N_{\mathrm{DFT}} = 32$, $h = 0.1/2\pi$, $A_s = 2$, modulation type: $M = 8$. The averaged results were obtained in 100 Monte Carlo trials where 500 CE-OFDM signals were produced for each trial.

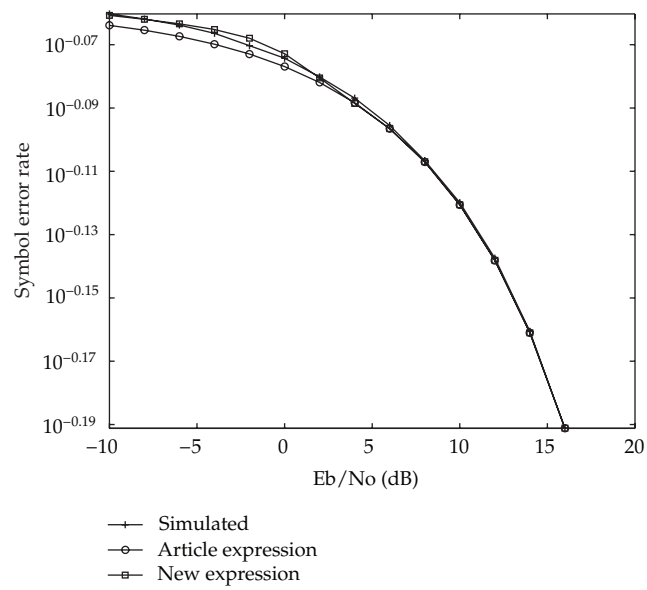

Figure 6: SER comparison as a function of E_b/N_0 between the simulated, new proposed expression (10) and the expression proposed by [5] given in (7). $N_{\mathrm{DFT}} = 8$, $h = 0.1/2\pi$, $A_s = 2$, modulation type: $M = 8$. The averaged results were obtained in 100 Monte Carlo trials where 500 CE-OFDM signals were produced for each trial.

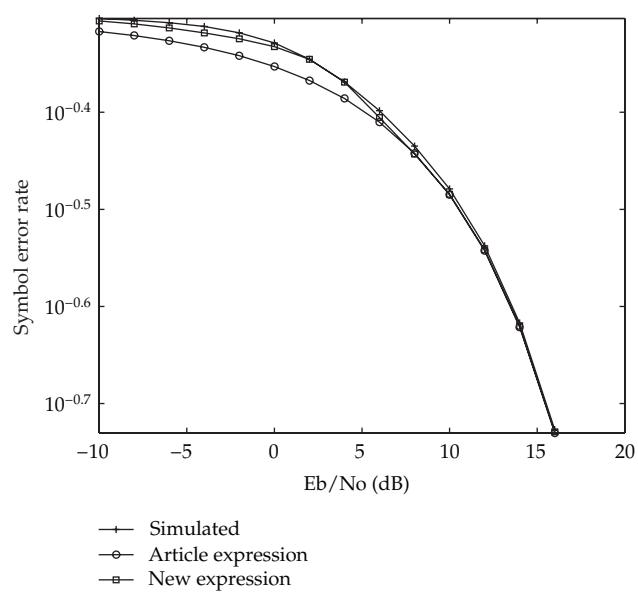

Figure 7: SER comparison as a function of E_b/N_0 between the simulated, new proposed expression (10) and the expression proposed by [5] given in (7). $N_{\mathrm{DFT}} = 64$, $h = 0.1/2\pi$, $A_s = 2$, modulation type: $M = 2$. The averaged results were obtained in 100 Monte Carlo trials where 500 CE-OFDM signals were produced for each trial.

those obtained by simulation. In the following, we denote the expression given in (7) as "Article Expression" and our new obtained expression for the SER (10) as "New Expression."

Figures 2, 3, 4, 5, and 6 show the performance comparison of the SER as a function of E_b/N_0 between our expression for the SER (10), the expression given in (7), and the simulated results for the $M = 8$ case with various values for the parameter h and DFT length N_{DFT}. Figures 7, 8, 9, 10, and 11 show the performance comparison of the SER as a function of E_b/N_0 between our expression for the SER (10), the expression given in (7), and the simulated results for the $M = 2$ case with various values for the parameter h and DFT length N_{DFT}. According to Figures 2 to 11, our expression

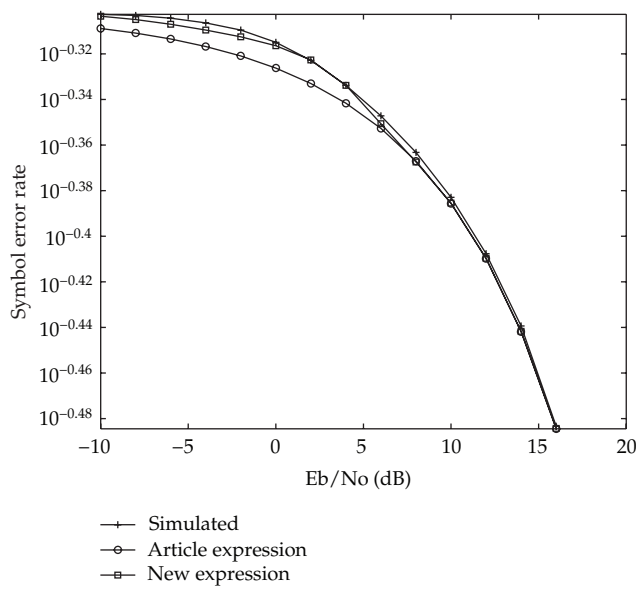

Figure 8: SER comparison as a function of E_b/N_0 between the simulated, new proposed expression (10) and the expression proposed by [5] given in (7). $N_{\mathrm{DFT}} = 64$, $h = 0.05/2\pi$, $A_s = 2$, modulation type: $M = 2$. The averaged results were obtained in 100 Monte Carlo trials where 500 CE-OFDM signals were produced for each trial.

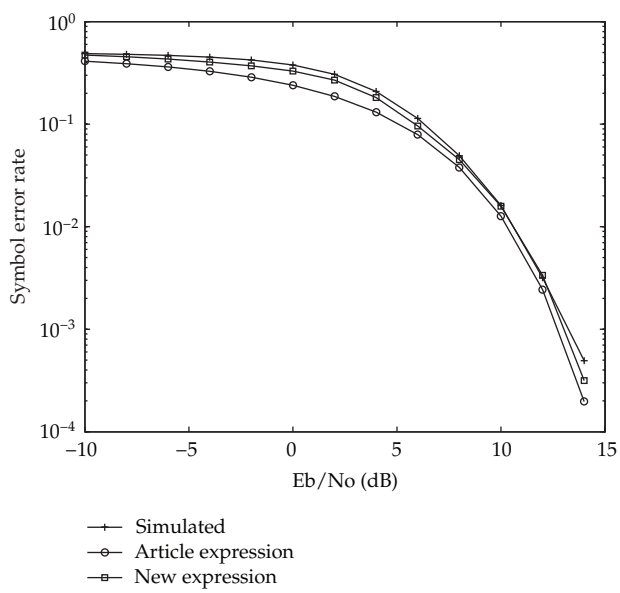

Figure 9: SER comparison as a function of E_b/N_0 between the simulated, new proposed expression (10) and the expression proposed by [5] given in (7). $N_{\mathrm{DFT}} = 64$, $h = 0.5/2\pi$, $A_s = 2$, modulation type: $M = 2$. The averaged results were obtained in 100 Monte Carlo trials where 500 CE-OFDM signals were produced for each trial.

for the SER (10) describes better the simulated results for the entire range of E_b/N_0 values compared with the expression given in (7).

Note that our obtained expression for the SER (10) was derived under the following condition of $\rho \to 0$ which is equivalent to $N_{\mathrm{DFT}}/N\log_2(M)(E_b/N_0) \to 0$ or

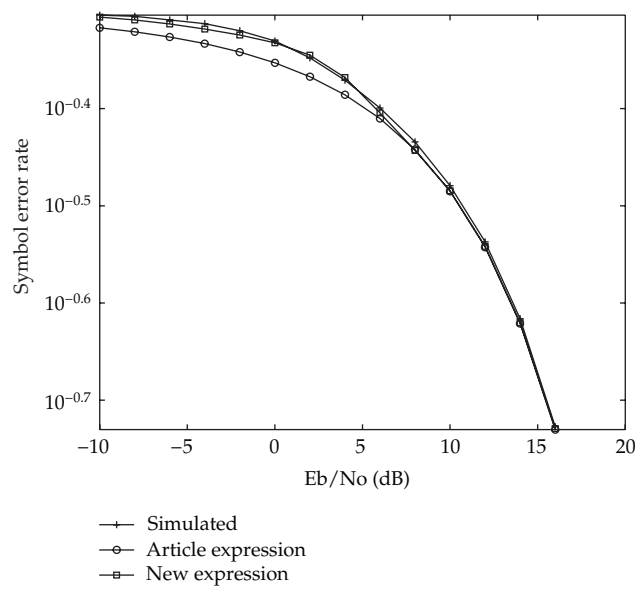

Figure 10: SER comparison as a function of E_b/N_0 between the simulated, new proposed expression (10) and the expression proposed by [5] given in (7). $N_{\mathrm{DFT}} = 32$, $h = 0.1/2\pi$, $A_s = 2$, modulation type: $M = 2$. The averaged results were obtained in 100 Monte Carlo trials where 500 CE-OFDM signals were produced for each trial.

$N\log_2(M)(E_b/N_0)/N_{\mathrm{DFT}} \to \infty$. The reason for having good results may be that, in practice, analysis based on low noise, which makes the Laplace integral and singular perturbation method feasible, can be extended to the region where the noise is not low. Note, for example, the papers [17, 18] where the Laplace integral and the singular perturbation method were applied under low noise assumption, and the results could be very well extended to the medium and high noise ranges. (As a matter of fact, these methods were rather successful, even in calculating the threshold region.) This is also the case in this paper, where good results are obtained even under the very low E_b/N_0 condition (Figures 2 to 11). In addition, it should not be forgotten that we have not approximated the pdf of the random variable $\xi[n]$ as a Gaussian pdf as was done in [5, 15] but rather used the exact expression (22). Although we used the Edgeworth expansion up to order four for approximating the pdf of $N[k]$ where satisfying results were obtained, it is possible that better results might be obtained when a higher order of the Edgeworth expansion is used.

5. Conclusion

In this paper, we presented a systematic approach for calculating the SER, applicable for CE-OFDM and for the AWGN case, which does not avoid the nonlinear problem caused by the phase demodulator as was done in [5, 15]. As a byproduct, a new expression was obtained for the SER that outperforms the recently proposed expression by [5, 15]. Although the SER performance difference between the new derived expression and the one proposed in [5, 15] is not very

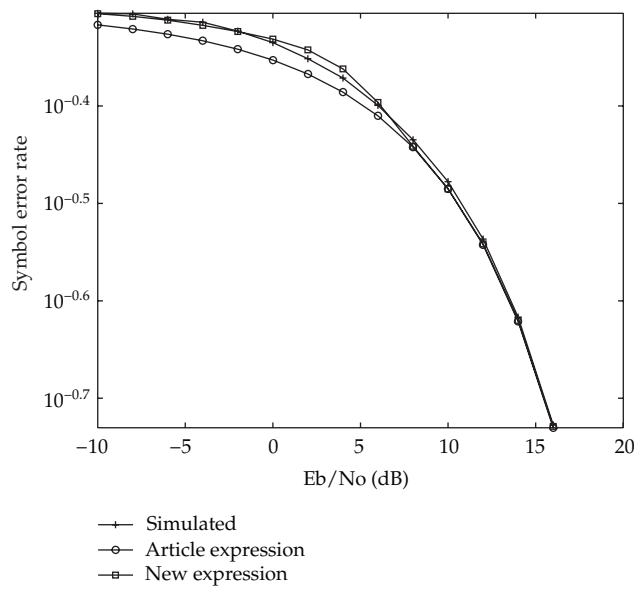

Figure 11: SER comparison as a function of E_b/N_0 between the simulated, new proposed expression (10) and the expression proposed by [5] given in (7). $N_{\mathrm{DFT}} = 8$, $h = 0.1/2\pi$, $A_s = 2$, modulation type: $M = 2$. The averaged results were obtained in 100 Monte Carlo trials where 500 CE-OFDM signals were produced for each trial.

high, it is still important from the mathematical point of view to have a systematic approach showing how to deal with the nonlinear problem. CE-OFDM was recently considered also for the power line communication channel where impulse noise is present. In future work, we intend to calculate the SER, applicable for CE-OFDM for the impulse noise case where the Symmetric Alpha Stable (SαS) Model is going to be used for statistical modelling of impulsive noise. Please note, the Cauchy distribution is a special case of the SαS distribution. It should be pointed out that the probability density function (pdf) of a SαS process in the presence of zero-mean Gaussian noise (designated SαS+ G) is a close approximation to the pdf of class B noise where by class B noise we mean the Middleton Class B Model which refers to impulsive noise with a spectrum that is broad compared to the receiver bandwidth [19]. Class B noise impulses produce transients in the receiver [19]. In addition, we also plan to use fractional Gaussian noise [20–22] instead of the additive white Gaussian noise we used in this paper for calculating the SER applicable for CE-OFDM. When using fractional Gaussian noise, we may consider the fluctuation range of E_b/N_0 and find if possible trivial fluctuations and nontrivial ones, methodologically referring to [21, 22] for references.

Acknowledgment

The authors would like to thank the anonymous reviewers for their fruitful and detail comments.

References

[1] European Telecommunications Standard, Radio Broadcast Systems, "Digital Audio Broadcasting to mobile, portable, and fixed receivers," preETS 300 401, 1994.

[2] U. Reimers, "DVB-T: the COFDM-based system for terrestrial television," *Electronics and Communication Engineering Journal*, vol. 9, no. 1, pp. 28–32, 1997.

[3] M. Pinchas and B. Z. Bobrovsky, "Analytic threshold calculation of frequency estimation for OFDM communication," *Signal, Image and Video Processing*, vol. 4, no. 2, pp. 187–195, 2010.

[4] C. Schurgers and M. Srivastava, "A systematic approach to peak-to-average power ratio in OFDM," in *Advanced Signal Processing: Algorithms, Architectures and Implementations XI*, vol. 4474 of *Proceedings of SPIE*, pp. 454–464, August 2001.

[5] S. C. Thompson, A. U. Ahmed, J. G. Proakis, J. R. Zeidler, and M. J. Geile, "Constant envelope OFDM," *IEEE Transactions on Communications*, vol. 56, no. 8, pp. 1300–1312, 2008.

[6] J. A. L. Silva, A. V. T. Cartaxo, and M. E. V. Segatto, "A PAPR reduction technique based on a constant envelope OFDM approach for fiber non- linearity mitigation in optical direct-detection systems," *Journal of the Optical Communications and Networking*, vol. 4, no. 4, pp. 296–303, 2012.

[7] R. Mohseni, A. Sheikhi, and M. A. Masnadi-Shirazi, "Multicarrier constant envelope OFDM signal design for radar applications," *International Journal of Electronics and Communications*, vol. 64, no. 11, pp. 999–1008, 2010.

[8] E. G. Mohammed, B. Jamal, and A. Benbassou, "Peak to average power ration reduction in OFDM system using constant envelope for transmission via PLC channel," in *Proceedings of the Electromagnetics Research Symposium (PIERS '11)*, pp. 1540–1544, Marrakesh, Morocco, March 2011.

[9] P. H. Moose, "Technique for orthogonal frequency division multiplexing frequency offset correction," *IEEE Transactions on Communications*, vol. 42, no. 10, pp. 2908–2914, 1994.

[10] A. N. D'Andrea, A. Ginesi, and U. Mengali, "Digital carrier frequency estimation for multilevel CPM signals," in *Proceedings of IEEE International Conference on Communications (ICC '95)*, pp. 1041–1045, June 1995.

[11] D. C. C. Bover, "Moment equation methods for nonlinear stochastic systems," *Journal of Mathematical Analysis and Applications*, vol. 65, no. 2, pp. 306–320, 1978.

[12] M. Pinchas and B. Z. Bobrovsky, "A novel HOS approach for blind channel equalization," *IEEE Transactions on Wireless Communications*, vol. 6, no. 3, pp. 875–886, 2007.

[13] S. A. Orszag and C. M. Bender, *Advanced Mathematical Methods for Scientists and Engineers*, International Series in Pure and Applied Mathematic, McGraw-Hill, New York, NY, USA, 1978.

[14] M. Pinchas and B. Z. Bobrovsky, "A Maximum Entropy approach for blind deconvolution," *Signal Processing*, vol. 86, no. 10, pp. 2913–2931, 2006.

[15] S. C. Thompson, *Constant envelope OFDM phase modulation [Ph.D. thesis]*, University of California, San Diego, Calif, USA, 2005.

[16] A. Papoulis, *Probability, Random Variables, and Stochastic Process*, International Student Edition, McGraw Hill Kogakusha, 1965.

[17] A. L. Welti and B. Z. Bobrovsky, "Mean time to lose lock for a coherent second-order PN-code tracking loop—the singular perturbation approach," *IEEE Journal on Selected Areas in Communications*, vol. 8, no. 5, pp. 809–818, 1990.

[18] B. Z. Bobrovsky and Z. Schuss, "A singular perturbation method for the computation of the mean first passage time in a nonlinear filter," *SIAM Journal on Applied Mathematics*, vol. 42, no. 1, pp. 174–187, 1982.

[19] S. A Bhatti, Q. Shan, I. A. Glover et al., "Impulsive noise modelling and prediction of its impact on the performance of WLAN receiver," in *Proceedings of the 17th European Signal Processing Conference (EUSIPCO '09)*, pp. 1680–1684, Glasgow, UK, August 2009.

[20] M. Li and W. Zhao, "On 1/f noise," *Mathematical Problems in Engineering*, vol. 2013, Article ID 673648, 2013.

[21] M. Li and W. Zhao, "Quantitatively investigating locally weak stationarity of modified multifractional Gaussian noise," *Physica A*, vol. 391, no. 24, pp. 6268–6278, 2012.

[22] M. Li, Y.-Q. Chen, J.-Y. Li, and W. Zhao, "Holder scales of sea level," *Mathematical Problems in Engineering*, vol. 2013, Article ID 863707, 2013.